Supporting Information

Bifunctional Oxygen Reduction/Evolution Reaction Electrocatalysts Achieved by Axial Ligands Modulation on Two-Dimensional Porphyrin Frameworks

Tianze Xu, Tianyang Liu* and Yu Jing*

Jiangsu Co-Innovation Centre of Efficient Processing and Utilization of Forest Resources, College of Chemical Engineering, Nanjing Forestry University, Nanjing 210037, China

Email: liutianyang@njfu.edu.cn; yujing@njfu.edu.cn

1. Computational details

S1.1 Constant-Potential Calculations

Via adjusting the work function, we changed the electric potential of electrochemical interface. It could be calculated by

$$U = (W_f - 4.60) + 0.0592 \times pH \quad \textbf{(S1)}$$

where U is electrode potential referenced to RHE, W_f is the work function and 4.60 is the work function of H_2/H^+ at standard conditions.[1,2] The work function could be controlled by altering the numbers of charges. When electrode potential at a fixed potential of RHE, electric potential referenced to SHE scale is also changed by the pH values. It was given by:

$$U_{RHE} = U_{SHE} + 0.0592 \times pH \quad \textbf{(S2)}$$

According to Neurock methods,[3] the potential-dependent energy can be calculated by:

$$\mathrm{E}(U) = E_{\mathrm{DFT}} + \int_0^{\mathrm{q}} \langle \mathrm{V}_{\mathrm{TOT}}^{-} \rangle \mathrm{dQ} + \mathrm{q}W_{\mathrm{f}} \quad \textbf{(S3)}$$

where E_{DFT} is the total energy of the unit cell calculated by DFT calculation, $\int_0^{\mathrm{q}} \langle \mathrm{V}_{\mathrm{TOT}}^{-} \rangle \mathrm{dQ}$ is an integral from 0 to the system charge of the average electrostatic potential in the unit cell, and $\mathrm{q}W_{\mathrm{f}}$ is given by the number of electrons (add and subtracted) multiplied by the work functions.

S1.2 pH- and Potential-dependent Thermodynamics and Kinetics Calculations

The reaction energy barrier was simulated by adopting the climbing-image nudged elastic band (CI-NEB) method,[4] the Poisson-Boltzmann implicit solvation model was used to consider solvation effect,[5,6] the cavity setting in VASPsol was turned off to avoid numerical instabilities.

The O_2 molecule diffusion, adsorption, and electrochemical steps for ORR equations (S1 to S6) and OER equcations (S7 to S11) were presented below:

$$\mathrm{O_2\ (aq)} \overset{k_1}{\underset{k_{-1}}{\rightleftarrows}} \mathrm{O_2\ (dl)} \quad \textbf{(S4)}$$

$$\mathrm{O_2\ (dl) + *} \overset{k_2}{\underset{k_{-2}}{\rightleftarrows}} \mathrm{O_2*} \quad \textbf{(S5)}$$

$$\mathrm{O_2 * + H^+ + e^-} \overset{k_3}{\underset{k_{-3}}{\rightleftarrows}} \mathrm{OOH*} \quad \textbf{(S6)}$$

$$\mathrm{OOH* + H^+ + e^-} \overset{k_4}{\underset{k_{-4}}{\rightleftarrows}} \mathrm{O* + H_2O} \quad \textbf{(S7)}$$

$$\mathrm{O* + H^+ + e^-} \overset{k_5}{\underset{k_{-5}}{\rightleftarrows}} \mathrm{OH*} \quad \textbf{(S8)}$$

$$\mathrm{OH* + H^+ + e^-} \overset{k_6}{\underset{k_{-6}}{\rightleftarrows}} \mathrm{H_2O + *} \quad \textbf{(S9)}$$

$$\mathrm{H_2O + *} \overset{k_7}{\underset{k_{-7}}{\rightleftarrows}} \mathrm{OH* + H^+ + e^-} \quad \textbf{(S10)}$$

$$OH^* \overset{k_8}{\underset{k_{-8}}{\rightleftarrows}} O^* + H^+ + e^- \quad \textbf{(S11)}$$

$$O^* + H_2O \overset{k_9}{\underset{k_{-9}}{\rightleftarrows}} OOH^* + H^+ + e^- \quad \textbf{(S12)}$$

$$OOH^* \overset{k_{10}}{\underset{k_{-10}}{\rightleftarrows}} O_2^* + H^+ + e^- \quad \textbf{(S13)}$$

$$O_2^* \overset{k_{11}}{\underset{k_{-11}}{\rightleftarrows}} O_2\,(aq) + * \quad \textbf{(S14)}$$

where k_i and k_{-i} are the rate constants of reaction and reverse reaction. According to the transition state theory, k_i and k_{-i} are calculated by:

$$k_i = A_i exp(-\frac{\Delta G^{\ddagger}}{k_B T}) \quad \textbf{(S15)}$$

$$k_{-i} = \frac{k_i}{K_i} \quad \textbf{(S16)}$$

where A_i is the effective prefactor and K_i is the equilibrium constant. Considering all the rate equations are at the steady state, then the relationship between U and coverage (θ) at pH = 1 and 13 can be obtained, and the current density is calculated by:

$$j = -2e\rho_{Co} TOF_{H_2O} \quad \textbf{(S17)}$$

S1.3 The formation energy E_f and dissolution potential U_{diss} calculations

The formation energy E_f and dissolution potential U_{diss} can be defined as:

$$E_f = E_{M-TEP} - E_M - E_{TEP} \quad \textbf{(S18)}$$

$$U_{diss} = U_{diss}^{o}(metal,bulk) - {E_f}/{ne} \quad \textbf{(S19)}$$

where E_M is the total energy of the metal atom in its most stable bulk structure, E_{M-TEP} and E_{TEP} are the total energies of substrate and substrate without metal center, U_{diss}^{o} and n are the standard dissolution potential of bulk metal and the number of electrons

involved in the dissolution, respectively.

2. Supporting Figures

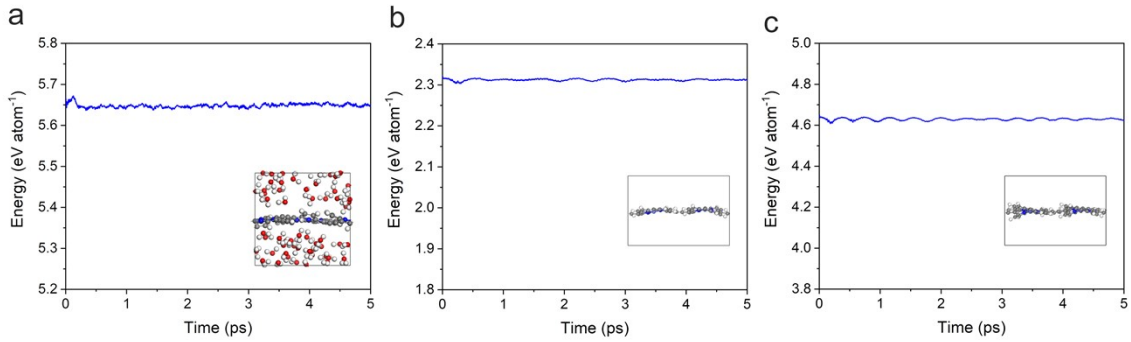

Figure S1. (a) Total potential energy fluctuation of 2D Co-TEP-COF at the end of a 5 ps ab initio molecular dynamic (AIMD) simulation at the temperature of 500 K. (b,c) Total potential energy fluctuation of 2x1x1 and 2x2x1 supercell at the end of a 5 ps ab initio molecular dynamic (AIMD) simulation at the temperature of 300 K.

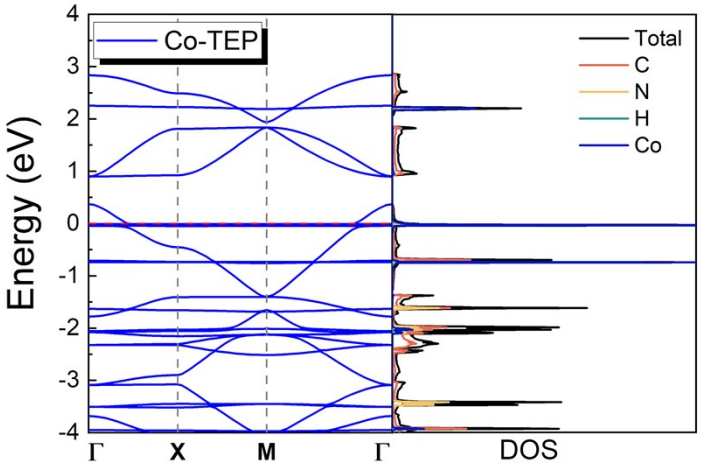

Figure S2. Band structure and density of states of 2D Co-TEP-COF.

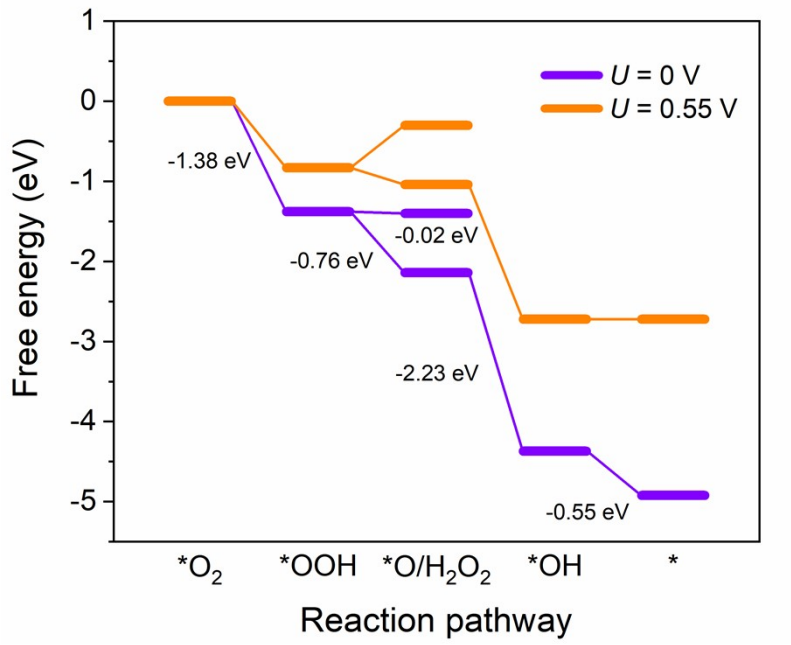

Figure S3. Free energy diagram for the ORR pathway on 2D Co-TEP COF.

.

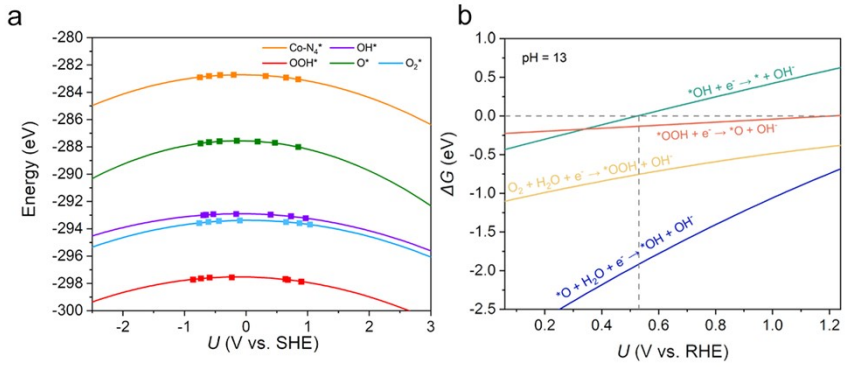

Figure S4. (a) The quadratic functions of the electrode potential *U* (V vs. SHE) and the total energy for 2D Co-TEP COF monolayer system. (b) Free energy changes for OER of 2D Co-TEP-CN COF monolayer at pH = 13 as a function of potential.

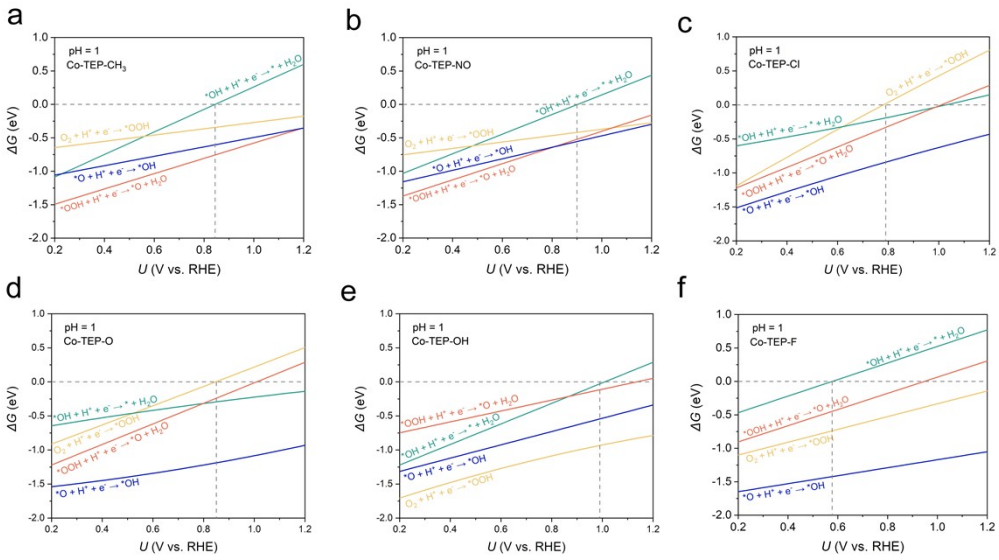

Figure S5. (a-f) Free energy changes for ORR of the 2D Co-TEP-X (X = O, OH, Cl, CH_3, NO, F) COFs at pH = 1 as a function of potential.

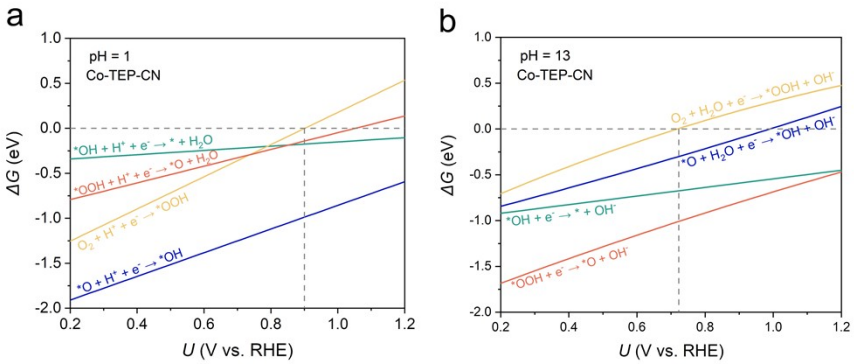

Figure S6. Free energy changes for ORR of 2D Co-TEP-CN COF monolayer at pH = 1 and 13 as a function of potential.

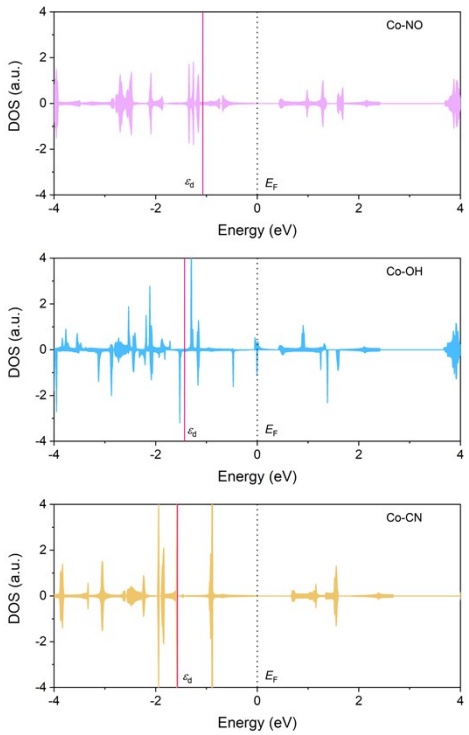

Figure S7. Density of states (DOS) of the 2D Co-TEP-X (X = NO, OH, CN) and their d-band center.

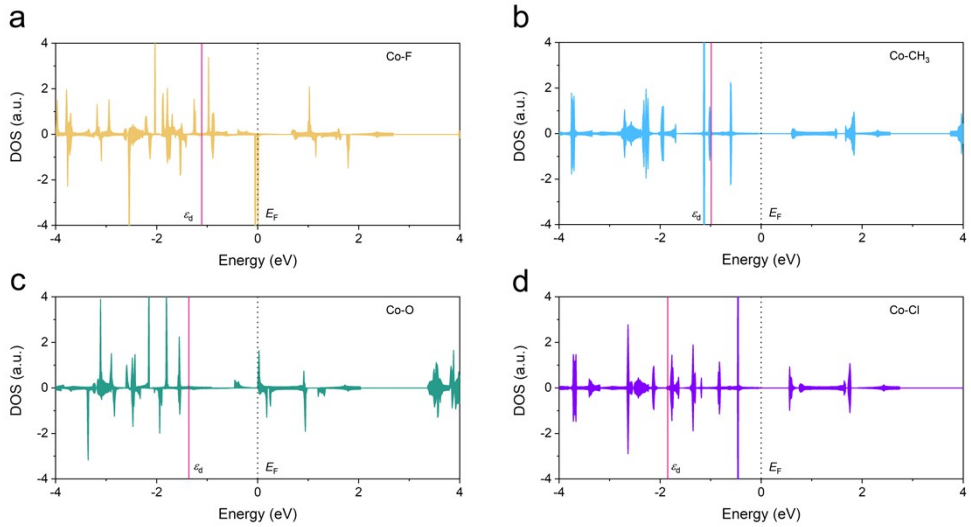

Figure S8. (a-d) Density of states (DOS) of the 2D Co-TEP-X (X = F, CH_3, O, Cl) and their d-band center.

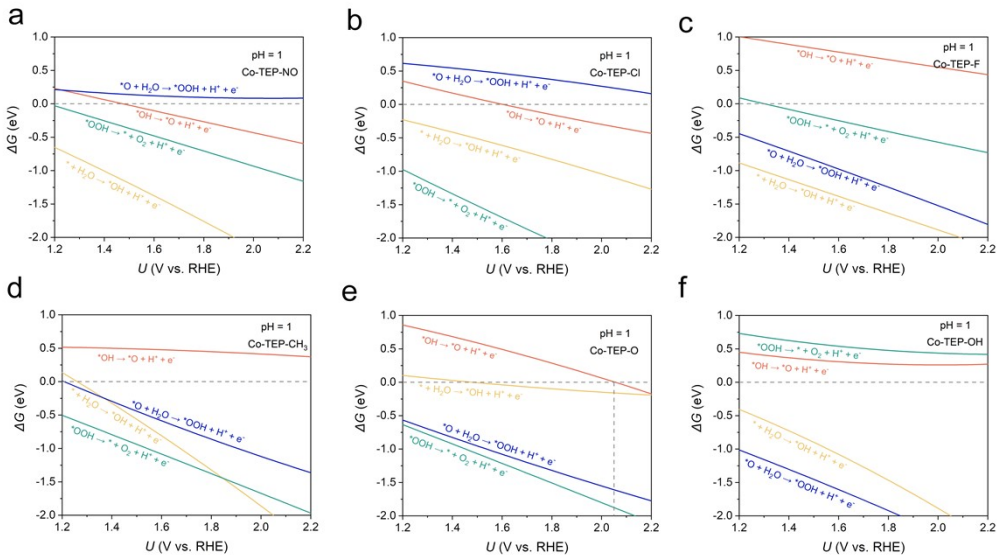

Figure S9. (a-f) Free energy changes for OER of the 2D Co-TEP-X (X = O, OH, Cl, CH3, NO, F) COFs at pH = 1 as a function of potential.

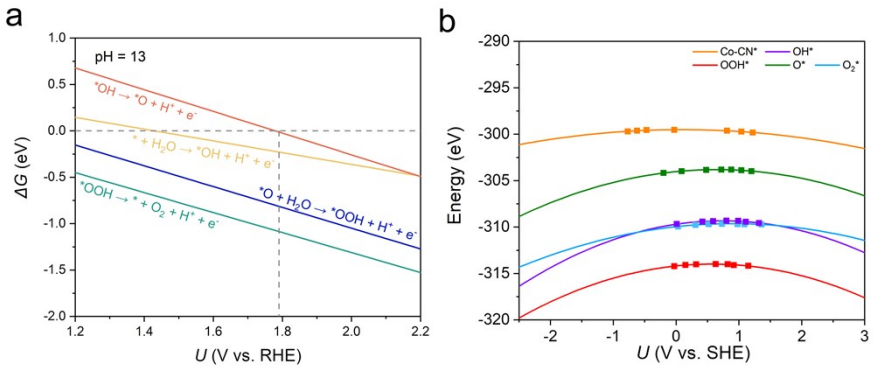

Figure S10. (a) Free energy changes for OER of 2D Co-TEP-CN COF monolayer at pH = 13 as a function of potential. (b) The quadratic functions of the electrode potential *U* (V vs. SHE) and the total energy for 2D Co-TEP-CN COF monolayer system.

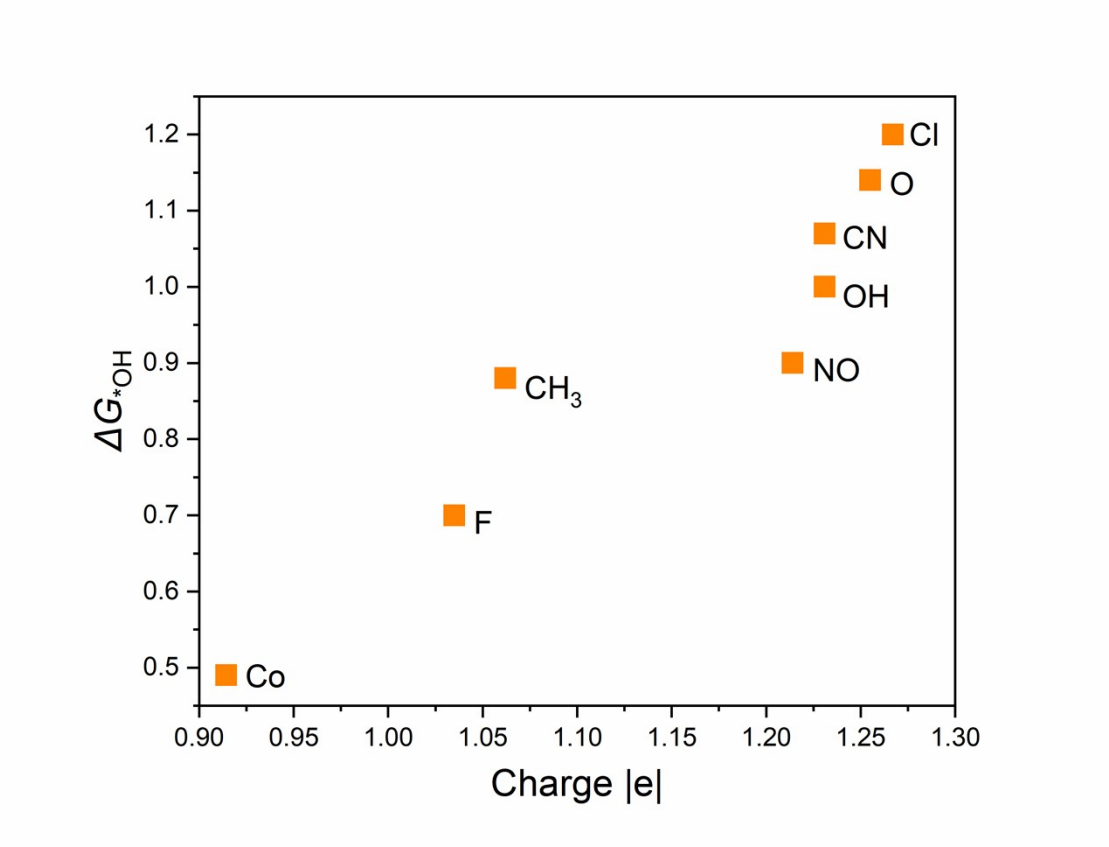

Figure S11. The relationship between calculated net charge values of Co in Co-TEP-X and the adsorption energy of *OH (ΔG_{*OH}).

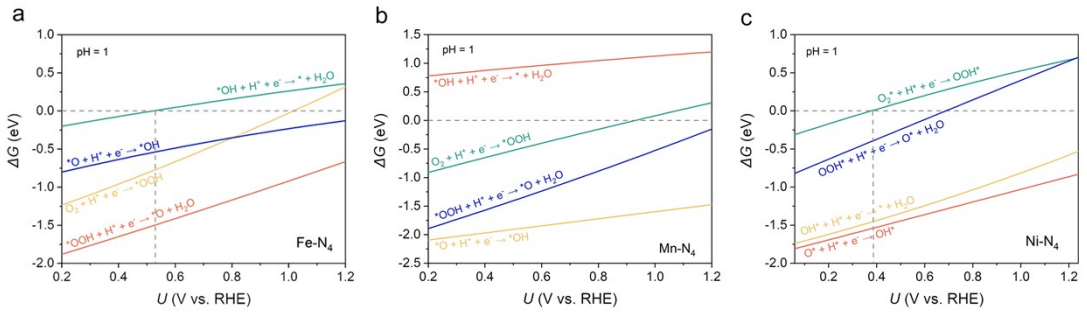

Figure S12. (a-c) Free energy changes for ORR of the 2D M-TEP COFs (M = Fe, Mn, Ni) at pH = 1 as a function of potential.

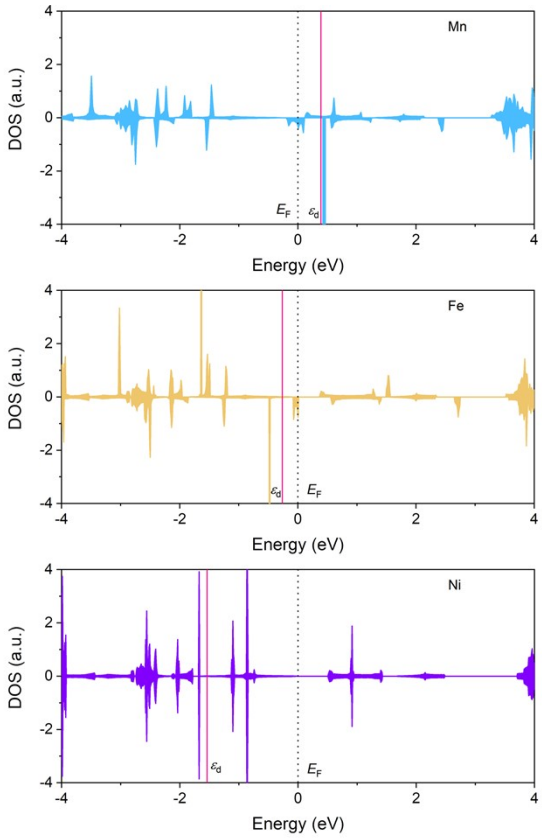

Figure S13. Density of states (DOS) of the 2D M-TEP COF (X = Mn, Fe, Ni) and their d-band center.

Table S1. Computed formation energy (E_f) and dissolution potential (U_{diss})of metals. For comparison, standard dissolution potential (U^0_{diss}) of metal atoms is also listed.

M	Cr	Mn	Fe	Co	Ni
E_f (eV)	-5.76	-5.34	-4.69	-4.57	-4.65
U^0_{diss}(V)	-0.91	-1.19	-0.45	-0.28	-0.26
U_{diss}(V)	1.97	1.48	1.90	2.01	2.07

POSCAR of Optimized 2D Co-TEP-COF

POSCAR
1.00000000000000
10.9499999999999993 0.0000000000000000 0.0000000000000000
0.0000000000000000 10.9499999999999993 0.0000000000000000
0.0000000000000000 0.0000000000000000 15.0000000000000000
C N H Co

24 4 8 1

Direct

0.4036136568969860	0.7555785151455066	0.4979554646360198
0.2886210811944596	0.8176413242337145	0.4980090807134385
0.2006686232759572	0.7298831879589948	0.4981430506158452
0.2625294057821775	0.6147374261743873	0.4981438681051820
0.5158604043262950	0.8173432026000308	0.4978031158495646
0.6280305303224523	0.7554455200866724	0.4976916079375195
0.7689512755702532	0.6144204357827212	0.4978137165811710
0.8309354446586246	0.7294782020622792	0.4974848734991708
0.7431048834366997	0.8173475548276574	0.4974022276636672
0.2625268709876143	0.3902402584986108	0.4980190635942953
0.2006974274203839	0.5024868777466340	0.4981585105158318
0.7689479237922202	0.3899246826254518	0.4981543943025197
0.8307712060716771	0.5021648347550777	0.4980577870432532
0.2005587717539197	0.2751618487760191	0.4978515875258094
0.2884063274629692	0.1873110493151585	0.4977026211048634
0.4034620902931061	0.2492286923526962	0.4978170616424507
0.8308092710155848	0.2747811335549344	0.4982709184547311
0.7428609976868006	0.1870222992189430	0.4981959295349065
0.6278690996625977	0.2490790540458561	0.4980362410412149
0.5156288499148716	0.1873091672596830	0.4978754233510674
0.5156357895979123	0.0582533570312628	0.4978222448089277
0.0716689117141903	0.5024227689346911	0.4982082050902293
0.9598157693646324	0.5022143474360983	0.4981512830788300
0.5158540292768378	0.9464004183205023	0.4977923074922616
0.3881503344386837	0.6300081029620425	0.4980259585763538
0.6433638199966373	0.6298483059896927	0.4978805873126450
0.3881254725130363	0.3748141085390059	0.4979748251794782
0.6433370942244869	0.3746473161308892	0.4980377461394113
0.1025529263578152	0.7413403068394173	0.4982119074104005
0.1024340608409819	0.2639047618086385	0.4978312540951311
0.2772661597341832	0.0891570534955685	0.4975432858224011
0.7538835436759654	0.0888522662142893	0.4982634513077968
0.2776014229176491	0.9158073924671144	0.4979305846330263
0.9290717843764318	0.7407006976355571	0.4972921364747138
0.7542842691929451	0.9154939110056537	0.4971225214063785
0.9289265703392556	0.2633434013261141	0.4983844735981330
0.5157539749126865	0.5023160798424163	0.4980006538613642

References

(1) Duan, Z.; Henkelman, G. Theoretical Resolution of the Exceptional Oxygen Reduction Activity of Au(100) in Alkaline Media. *ACS Catal.* **2019**, *9* (6), 5567-5573.

(2) Duan, Z.; Henkelman, G. Surface Charge and Electrostatic Spin Crossover Effects in CoN_4 Electrocatalysts. *ACS Catal.* **2020,** *10* (20), 12148-12155.

(3) Filhol, J. S.; Neurock, M. Elucidation of the Electrochemical Activation of Water Over Pd by First Principles. *Angew. Chem. Int. Ed.* **2006**, *118*, 416−420

(4) Henkelman, G.; Uberuaga, B. P.; Jónsson, H. A Climbing Image Nudged Elastic Bband Method for Finding Saddle Points and Minimum Energy Paths. *J. Chem. Phys.* **2000**, *113* (22), 9901-9904.

(5) Mathew, K.; Sundararaman, R.; Letchworth-Weaver, K.; Arias, T. A.; Hennig, R. G. Implicit Solvation Model for Density-Functional Study of Nanocrystal Surfaces and Reaction Pathways. *J. Chem. Phys.* **2014**, *140* (8), 084106.

(6) Mathew, K.; Kolluru, V. S. C.; Mula, S.; Steinmann, S. N.; Hennig, R. G. Implicit Self-Consistent Electrolyte Model in Plane-Wave Density-Functional Theory. *J. Chem. Phys.* **2019,** *151* (23), 234101.